Field-induced transitions in low-dimensional antiferromagnets and in a spin-peierls system

Jongh, L.J. de; Brom, H.B.; Groot, H.J.M. de; Hijmans, T.W.; Korving, W.H.

Journal of Magnetism and Magnetic Materials 54-57 (1986) 1447-1452

FIELD-INDUCED TRANSITIONS IN LOW-DIMENSIONAL ANTIFERROMAGNETS AND IN A SPIN-PEIERLS SYSTEM

L.J. de JONGH, H.B. BROM, H.J.M. de GROOT, Th.W. HIJMANS and W.H. KORVING

Kamerlingh Onnes Laboratory, State University of Leiden, P.O. Box 9502, 2300 RA Leiden, The Netherlands

Field-induced transitions in weakly anisotropic low-d antiferromagnets provide a rich field of critical phenomena, closely related to topics outside magnetism. We discuss phase diagrams for quasi 1-d and 2-d antiferromagnets, which relate to 1-d solitons, the 2-d commensurate–incommensurate (C–IC) transition, the Kosterlitz–Thouless transition and the random-field problem. We also review (and present new) experimental data on the Spin–Peierls compound in TTF–AuBDT in the light of current theory. At low temperatures a field-induced C–IC transition to a soliton-lattice phase is predicted, which is confirmed by our data.

1. Introduction

Field-induced transitions in low-dimensional (low-d) antiferromagnets provide a rich and interesting field of critical phenomena, that remains still largely unexplored. We briefly review a number of studies recently performed within our group. Firstly we consider the behavior for quasi 1-d and quasi 2-d antiferromagnets with weak antisotropy and no coupling to the lattice [1,2]. Subsequently we discuss field-dependent studies [3–6] on the Spin–Peierls system TTF–$AuC_4S_4(CF_3)_4$ (TTF–AuBDT), where we study the dimerization instability of a system of antiferromagnetic Heisenberg chains that are spin–phonon coupled to the 3-d crystal lattice.

2. Phase-diagrams of low-d antiferromagnets

The discussion in this section is based on the Hamiltonian

$$\mathscr{H} = -2\tilde{J}\sum_{\langle i,j\rangle} \boldsymbol{s}_i\cdot\boldsymbol{s}_j - \sum_k \left\{ \tilde{D}_x s_{kx}^2 - \tilde{D}_z s_{kz}^2 + g\mu_B S\boldsymbol{B}\cdot\boldsymbol{s}_k \right\} \tag{1}$$

Here $\tilde{J} = JS(S+1)$ and $J<0$, $\tilde{D}_x = D_x S(S+1)$ and $D_x > 0$, $\tilde{D}_z = D_z S(S+1)$ and $D_z > 0$. The $\boldsymbol{s}_i$ are unit vectors and summation is over nearest neighbor pairs. The $\tilde{D}_z$ term establishes a planar (XY) anisotropy, whereas the $\tilde{D}_x$ term singles out the X-axis as the preferential axis (Ising-type anisotropy).

We first recall current ideas about the phase diagram for the 3-d case (fig. 1a). We specialize to the uniaxially symmetric case by taking $\tilde{D}_z = 0$ in (1) and put the magnetic field parallel to the easy axis ($\boldsymbol{B} = \boldsymbol{B}_x$). The resulting phase diagram is sketched in fig. 1a. At low temperatures a 1st-order spin fop (SF) transition occurs at a critical field B_{sf} at which the moments flop from the easy axis to the perpendicular orientation. This is because for $B_x > B_{sf}$ the difference in Zeeman energy, $\frac{1}{2}(\chi_\perp - \chi_\parallel)B_x^2$, between perpendicular and parallel orientation exceeds the anisotropy energy $\tilde{D}_x$ that favours the X-axis (in an antiferromagnet one has $\chi_\parallel \ll \chi_\perp$ at low temperatures). The value for B_{sf} follows from $\tilde{D}_x = \frac{1}{2}(\chi_\perp - \chi_\parallel)B_{sf}^2$. At (much) higher fields a 2nd-order transition to the paramagnetic phase occurs (saturation field at $T = 0$). We denote the different phase by P (paramagnetic), I (ordered Ising-type) and XY (ordered planar of XY-type), and the boundaries by I–P, XY–P and I–XY. In 3-d antiferromagnets the 1st-order spin-flop line I–XY bifurcates in the 2nd-order I–P and XY–P lines at the bicritical point (B_2, T_2).

The features of the 3-d phase diagram are confirmed by experiments on e.g. $GdAlO_3$, $MnCl_2\cdot 4H_2O$ and MnF_2. In particular, the 1st-order character of the SF transition has been confirmed [7], provided that corrections are made for dipolar interactions not included in Hamiltonian (1) (demagnetizing effects).

We next discuss the quasi 2-d and quasi 1-d antiferromagnets, for which the phase-diagrams are found to be quite different (fig. 1b,c). In both cases the "spin-flop" no longer corresponds with a 1st-order transition, and also the nature of the other phase boundaries is different. We have recently shown [1,2] that good insight in the underlying physics is obtained on basis of the concept of *the effective field-dependent anisotropy*, $\tilde{D}_{eff}(B_x)$, which arises from the competition between the Zeeman energy and the anisotropy terms in Hamiltonian (1). For the uniaxial case $\tilde{D}_{eff}(B_x)$ is simply given by: $\tilde{D}_{eff}(B_x) = \tilde{D}_x - \frac{1}{2}(\chi_\perp - \chi_\parallel)B_x^2$. Using $\tilde{D}_x = \frac{1}{2}(\chi_\perp - \chi_\parallel)B_{sf}^2$ one immediately obtains:

$$\tilde{D}_{eff}(B_x) = \tilde{D}_x\left(1 - B_x^2/B_{sf}^2\right). \tag{2}$$

Since $\tilde{D}_{eff}(B_x)$ becomes zero and changes sign at $B_x = B_{sf}$, the behavior for the 2-d case is the following. For $B_x \uparrow B_{sf}$ one has a 2-d Heisenberg system with vanishing Ising-type anisotropy. The I–XY and the I–P phase boundaries become a single line of 2nd-order transitions, representing the decrease to zero with vanishing anisotropy [8] of the anisotropy-induced T_c of the weakly anosotropic 2-d Heisenberg antiferromagnet. We recall that for the 3-d case the zero-anisotropy limit obtained at $B_x = B_{sf}$ corresponds with a finite T_c, namely the

0304-8853/86/$03.50 © Elsevier Science Publishers B.V.

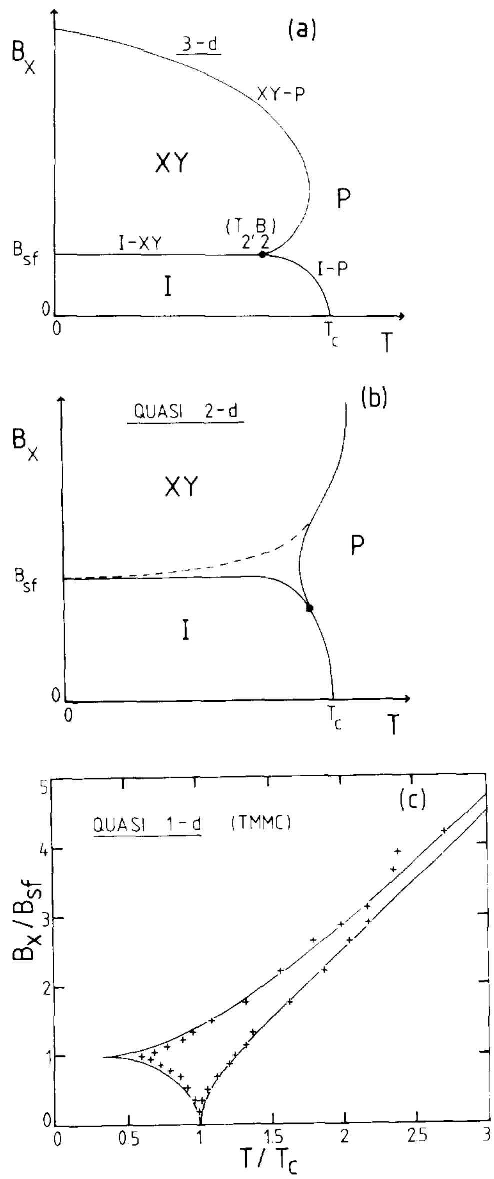

Fig. 1. Phase diagrams of weakly anisotropic Heisenberg antiferromagnets: (a) 3-d; (b) quasi 2-d; (c) quasi 1-d.

bicritital point. This is because the 3-d Heisenberg antiferromagnet does have a finite T_c, and therefore $T_2 = T_c^{\mathrm{Heis}} \neq 0$. However the 2-d Heisenberg model has no transition at $T \neq 0$, so that $T_2 = T_c^{\mathrm{Heis}} = 0$.

For fields $B_x > B_{sf}$ one has $\tilde{D}_{\mathrm{eff}}(B_x) < 0$, corresponding to a planar-type anisotropy that increases with field. This part of the phase diagram should therefore be identical to that of the isotropic Heisenberg antiferromagnet in a magnetic field [9]. The $T_c(B_x)$ rapidly increases for $B_x > B_{sf}$ from $T = 0$ towards the T_c-value of the 2-d XY model (dashed curve in fig. 1b). But before reaching this the curve will bend backwards due to saturation effects occurring in high fields ($g\mu_B B_x \simeq |\tilde{J}|$). We note that the XY–P boundary in this case corresponds with a line of Kosterlitz–Thouless transitions.

Except for the behavior for $B_x \downarrow B_{sf}$ (dashed curve), these ideas are well confirmed by the experimental phase diagrams of K_2MnF_4 [10] and $Mn(HCOO)_2 \cdot 2H_2O$ [11], which approximate the 2-d Heisenberg antiferromagnet with $S = 5/2$. For K_2MnF_4 the I–P and I–XY boundaries indeed form a continuous curve, that is fully described by theoretical predictions on basis of the above model. For $Mn(HCOO)_2 \cdot 2H_2O$ also the full XY–P boundary is available experimentally. The SF-transition in 2-d antiferromagnets is in all cases found to be of 2nd-order [1,2,10] in contrast with the 3-d antiferromagnets [7]. Similarly broad SF behavior occurs in quasi 1-d antiferromagnets [12]. There an explanation can be given in terms of excitation of 1-d soliton-pair states, which contribute to the magnetization and destroy the 1st-order character (see below). Therefore we have tried [1,2] to explain the broadening of the spinflop in quasi 2-d systems also in terms of domain wall-type excitations. In 2-d one has to consider the possibility of large, meandering domain walls, besides the small droplet-like excitations. We found close relationships between the 2-d antiferromagnet in a field and such problems as the 2-d commensurate–incommensurate transition, the Kosterlitz–Thouless transition and the massive Thirring model. However, it turns out [1,2] that the excitation energies of any of these nonlinear excitations, are too high to explain the observed broadening at very low temperatures. We finally arrived at an explanation in terms of random fields, arising from small amounts of lattice imperfections or impurities in the samples. It is predicted [13] that such random fields may effectively destroy the 1st-order character of a transition through the creation of domain walls. Our finding that this occurs in the quasi 2-d systems and not in the 3-d antiferromagnets would put the lower critical dimensionality for the random field problem at $d_c = 2$ [14]. We found that the observed exponential broadening of the spinflop in K_2MnF_4 could be well explained in such terms, assuming a concentration of imperfections of about 10^{-3}, which appears to be reasonable.

Finally, we return to the peculiar bifurcation behavior (fig. 1b) of the I–P into the I–XY and XY–P boundaries, as observed in both $Mn(HCOO)_2 \cdot 2H_2O$ [11] and K_2MnF_4 [10]. This phenomenon cannot be explained in terms of the effective anisotropy model and probably also arises from random field effects [1,2]. Recent theoretical work [15] on weakly anisotropic 2-d systems with random fields or anisotropies points to the possible existence of a glassy or floating phase in between the I- and P-phases. The floating phase may only exist for broad walls (as is the case for $B_x \simeq B_{sf}$), since these are not pinned by defects. Then the bifurcation might correspond with a Lifshitz point. A similar behavior has also been observed in a 3-d diluted antiferromagnet [7].

We next discuss the behavior in the quasi 1-d antiferromagnet $[(CH_3)_4]MnCl_3$ (TMMC) shown in fig. 1c. Since the pure 1-d antiferromagnet has no finite T_c, irrespective of the symmetry of the Hamiltonian, the observed transition is due to the weak interchain coupling J'. Nevertheless, the value of T_c is directly related to the 1-d correlation length $\xi_{1d}(T)$ along the chain, as follows from the relation $k_B T_c \simeq |\tilde{J}'| \xi_{1d}(T_c)$, which equates the thermal energy at T_c to the interaction energy between correlated chain segments on adjacent chains. It is found experimentally [16,17] that T_c varies extremely strongly with field (fig. 1c), which is explained as follows. For TMMC the anisotropy at temperatures close to T_c is described by an easy XY plane (eq. (1)), with the moments mainly along X for $B < B_{sf}$ (fig. 2a) and along Y for $B > B_{sf}$ (fig. 2b). In this field range the symmetry is thus planar with a weak inplane Ising anisotropy that vanishes at B_{sf}. The symmetry-breaking Ising component allows the thermal excitation of solitons (domain walls, kinks), which are transition-regions between domains corresponding to the interchange of the two antiferromagnetic sublattices (fig. 2a,b). The presence in TMMC of these excitations has been well-established by e.g. NMR and neutron scattering experiments [17].

Since the kinks drastically affect the correlation length, we may put $\xi_{1d} = 1/2n_s$, with n_s the soliton density $n_s = 2\sqrt{2/\pi}\,(E_s/k_B T)^{1/2} \exp(-E_s/k_B T)$. For the antiferromagnet the soliton excitation energy on basis of eqs. (1) and (2) is $E_s = 4|\tilde{J}\tilde{D}_{eff}(B)|^{1/2}$, which vanishes at B_{sf}. The exponential in n_s explains the drastic dependence of T_c on B, since $T_c \propto \xi_{1d} \propto 1/n_s$. This simple relation reproduces the relative variation of $T_c(B)$ for TMMC very well (fig. 1c), where $T_c(0)$and B_{sf} follow from experiment.

For the quasi 1-d antiferromagnets the SF-transition is not 1st-order. An explanation in terms of the soliton model [1,2,18,19] is based upon the excitation of wall-pairs in the ordered phase, as sketched in fig. 2c. As in the above, the energy $2E_s$ of the pairs will decrease for $B \to B_{sf}$, so that their density and wallwidth $d_s = |\tilde{J}/\tilde{D}_{eff}(B)|^{1/2}$ will increase. Since the moments rotate over the wallwidth, the wall-pair states contribute to the magnetization and thereby the 1st-order character of the SF-transition (discontinuous jump) is destroyed. With this model the observed [12] SF-transition in K_2FeF_5 can be well accounted for [1,2]. We finally note that our wall-pair-state model is in agreement with the droplet theory of Bruce and Wallace [20] for dimension $d = 1 + \delta$ in the limit $\delta \to 0$.

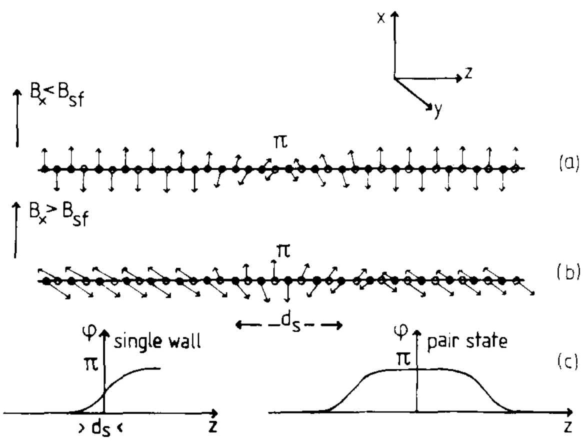

Fig. 2. Solitons in the quasi 1-d antiferromagnet.

3. Phase diagram of the Spin–Peierls system TTF–AuBDT

The Spin–Peierls (SP) transition has been observed in only a few quasi 1-d Heisenberg antiferromagnets (with $S = \frac{1}{2}$). It is the magnetic analogue of the regular Peierls transition in a 1-d metal (for reviews see e.g. refs. [19,21–23]). By introducing a coupling between the spins and the surrounding lattice (3-d phonon field) the antiferromagnetic chain is rendered unstable to spontaneous dimerization below the SP transition temperature T_{SP}. Theory predicts that on applying a magnetic fied the distortion wave vector remains fixed at the dimerization value π/a up to a critical field $B_c \approx k_B T_{SP}/g\mu_B$. Above B_c and at low temperatures the system is predicted to pass via an intermediate high-field phase from the dimerized into the paramagnetic phase. For the nature of this intermediate phase several proposals have been made. Recent theories [24–28] predict an incommensurate phase (soliton lattice) so that the transition at B_c is a commensurate–incommensurate (C–IC) transition (with commensurate the dimerized chain is meant). It is of interest to recall the analogy between the SP-transition and the regular Peierls transition [21,22], which becomes evident by mapping the Heisenberg Hamiltonian onto that of a chain of interacting spinless fermions by the Jordan–Wigner transformation. The variation of B then corresponds with a change in the chemical potential, and hence in the number of particles. Thus the SP transition in a magnetic field offers the unique possibility of investigating Peierls-type transitions as a function of bandfilling. Again there are close connections with other physical systems like solitons in polyacetylene, the lock-in transition in the 1-d quantum Sine–Gordon system (or the 2-d classical Sine–Gordon system), and the antiferromagnetic spin-flop transition.

Due to its low $T_{SP} = 2.03$ K, and the correspondingly low $B_c = 2.26$ T, the compound TTF–AuBDT is particularly suited for such field dependent studies. Our group has performed field-dependent specific heat, magnetic susceptibility, pulse-NMR and magnetization measurements [3–6]. In fig. 3 we show the experimental

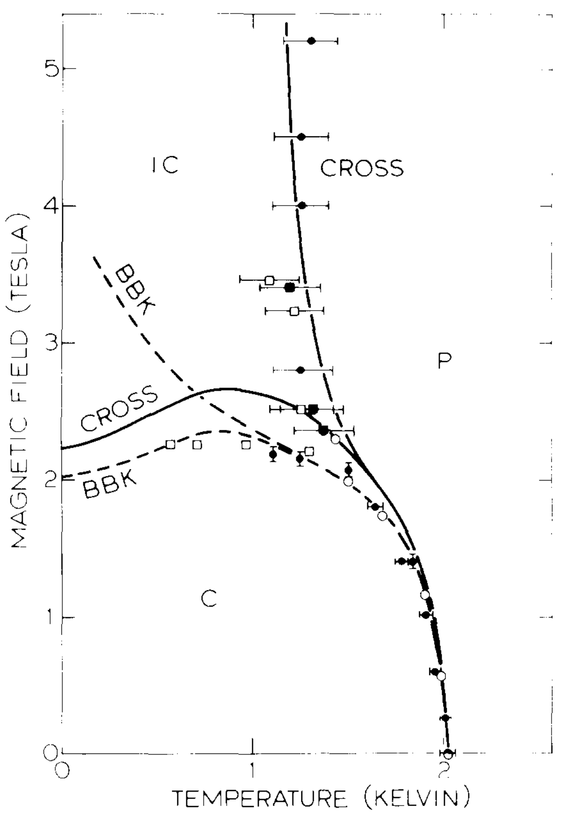

Fig. 3. Experimental phase diagram for TTF–AuBDT as obtained from χ-data (● – ref. [3] and new results), specific heat (○ – refs. [4,5]), NMR-relaxation (■ – refs. [5,6]) and NMR-linewidth (□ – refs. [5,6]).

phase diagram and compare it with theoretical predictions by Bulaevskii et al. (BBK) [29] and by Cross [30]. The latter theory is in good agreement with the experiment. The phases in the diagram are the paramagnetic (P) phase, the (dimerized) commensurate (C) phase, and the incommensurate (IC) phase. In fig. 4a we show the inverse HWHM of the proton spin-echo in the pulse-NMR experiment [6] as a function of field at $T = 0.57$ K and $T = 1.35$ K. The low-T data show a sharp transition around $B_c = 2.26$ T accompanied with some hysteresis (0.04 T). Similar jumps were seen up to 1.0 K, whereafter the transition becomes less abrupt, as seen for $T = 1.35$ K in fig. 4a. This would indicate that the transition becomes 1st-order below about 1 K. The shape of the echo-signal at $T = 1.0$ K for various fields around B_c shown in fig. 4a agrees with this idea, since the echo-signal appears to be composed of a broad and a narrow component over an interval of 0.04 T around B_c, suggesting the coexistence of two phases.

We recall that the echo-shape is the Fourier transform of the inhomogeneous part of the lineshape, as caused by the local fields exerted by the electron spins of the TTF molecules on the proton spins. By calculating the line-shape for different possible spin-configurations and comparing it with the experiment, information on the magnetic structure of the high-field phase is obtained. We have shown [6] that the echo-shape for $B > B_c$ is in good agreement with what is calculated for the soliton-lattice model of Nakano and Fukuyama [24]. In their model a C–IC transition occurs at B_c, above which the system is described by domains of dimerized regions separated by walls over which the lattice is incommensurate. Each wall carries a net spin $\frac{1}{2}$ pointing parallel to the field, such that the wall density is determined by the value of the magnetization (at $T = 0$ only the walls contribute to M). Apart from the net spin $\frac{1}{2}$ there is also associated with each soliton a non-vanishing staggered magnetization. We have argued that the latter in fact gives the dominant contribution to the NMR linewidth [6]. In the theory there is no consensus on whether the C–IC transition is 1st- or 2nd-order, whereas the P–IC transition from the paramagnetic phase is 2nd-order. Experimentally, broad transitions are observed along the P–IC line in both the spin-echo width (fig. 4b) and in the differential susceptibility χ (fig. 5a). So broad in fact that it is not possible to say experimentally whether it is 2nd- or higher order. The C–IC transition appears to be 1st-order on basis of the NMR data, but 2nd-order on basis of the magnetization (see fig. 5b, and below).

For some time we have even put in doubt whether the χ maxima observed at the P–IC line did indicate a true phase transition at all [3,18,19]. This arose e.g. from time-dependent effects which emerged from a comparison of the ac χ measured at 1880 Hz and the isothermal (static) χ derived from the $M(B)$ curve measured at 1.10 K [3]. These effects prompted us to extend the measurements of χ and M to lower temperatures, and some of our latest results are shown in figs. 5a,b. Quite surprisingly the ac χ curves shown are independent of the frequency in the covered range of 18–1880 Hz, although in the IC-phase the differential χ is much smaller than the static χ. This indicates a relaxation effect with an extremely small relaxation frequency (i.e. lower than 1 Hz, but larger than 0.01 Hz since time-effects larger than 100 s have not been seen in the magnetization studies).

Such extreme relaxation effects are compatible though with the soliton-lattice picture for the IC-phase. We recall that the value of M determines the density of domain walls, so that to obtain a variation ΔM by a field variation ΔB, a change Δn_s of the soliton density is needed. To obtain such a Δn_s in the experimental molecular crystal may very well imply a large time constant [27]. From the nature of the SP-transition it is highly probable that domain walls in adjacent chains are coupled to form planar-type walls extending over large distances. Further, to arrive at the discommensurations across the wall width implies the tilting of large

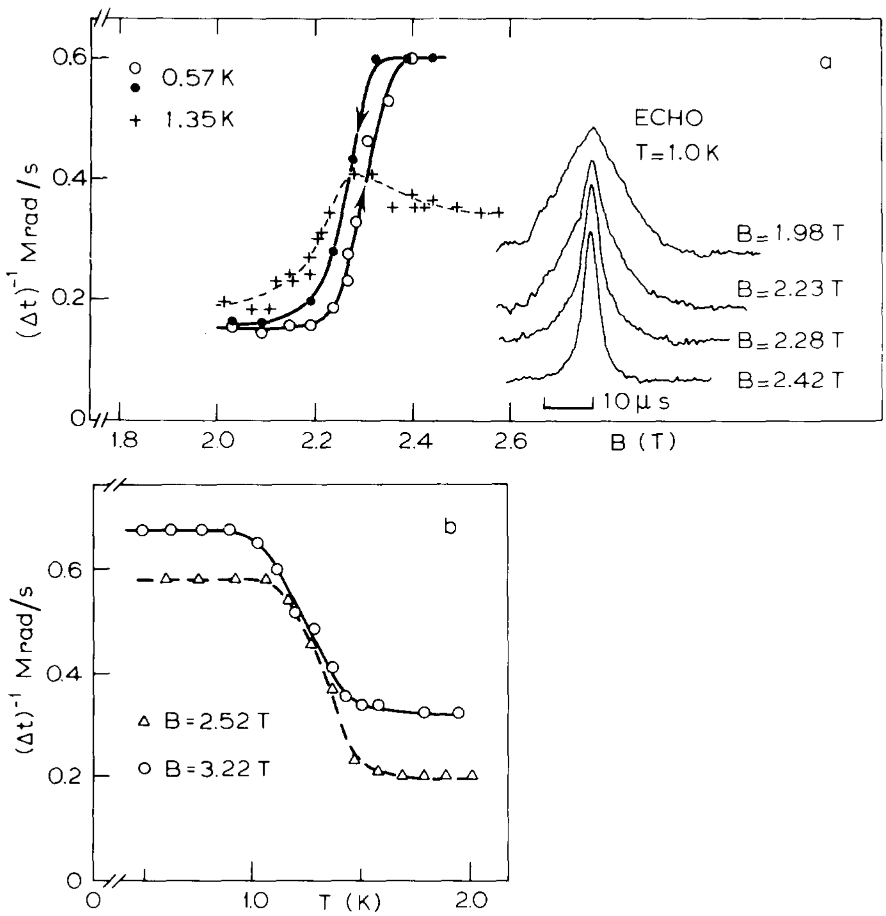

Fig. 4. The inverse half-width of the proton spin-echo in TTF–AuBDT. (a) vs. field; (b) vs. temperature. Inset in (a) shows echo-shape near $B_c = 2.26$ T at $T = 1.0$ K.

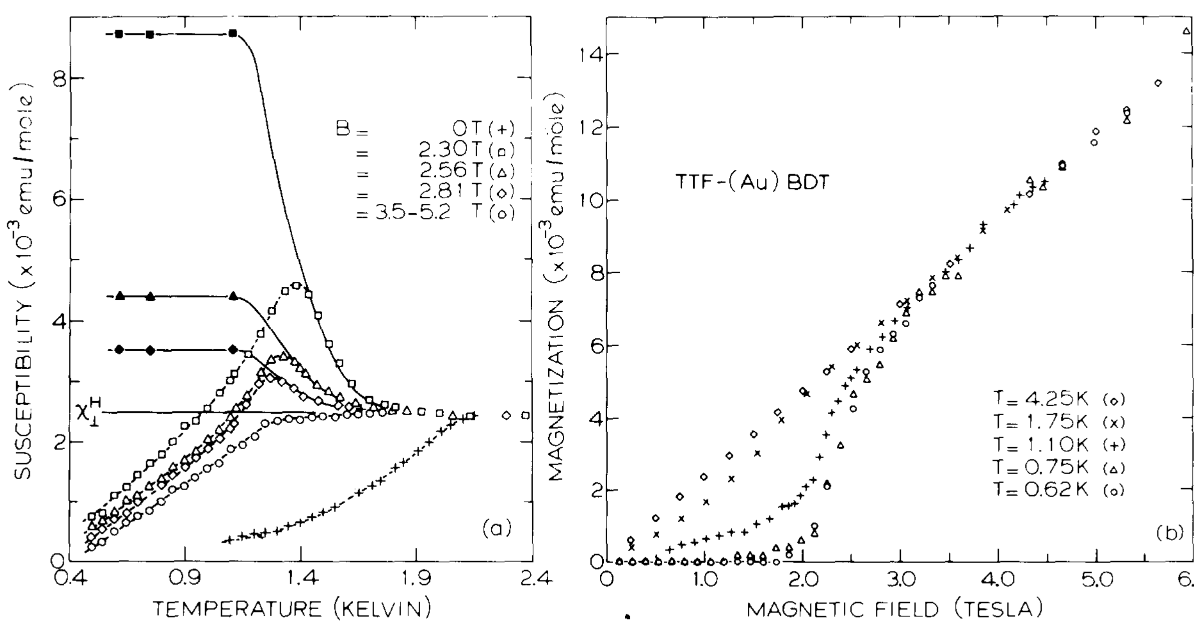

Fig. 5. Susceptibility vs. temperature (a) and magnetization vs. field (b) for TTF–AuBDT. Data for $B = 0$ (a) and $T = 1.10$, 1.75 and 4.25 K (b) are from ref. [3]. ($\chi_{\perp}^{H}$ is the theoretical susceptibility for the uniform antiferromagnetic Heisenberg chain.) In (a) closed symbols represent the static χ whereas open symbols refer to the differential χ for $\nu = 18$–1880 Hz.

organic molecules. It is thus conceivable that a Δn_s entails large time constants (see also ref. [27]).

From the $M(B)$ curves in fig. 5b it can be concluded that the static χ for $B > 3$ T is nearly independent of temperature in both the IC and the P phase. Only for fields closer to B_c temperature dependent effects are seen. This has been confirmed in isofield runs of M versus temperature. The conclusion is that for $B > 3$ T the static χ and M are almost insensitive to the I–U transition. The knee observed in fig. 5a for a field of 5.2 T is therefore only due to the time-dependent effects mentioned above. The general appearance of the $M(B)$ curves would agree with a 2nd-, rather than with a 1st-order C–IC transition. However, similar smooth curves were observed [19,22] for TTF–CuBDT, which nevertheless show accompanying hysteresis. We observed no hysteresis for TTF–AuBDT in the $M(B)$ curves, but since it is probably small (0.04 T) on basis of the NMR results, it may have gone unnoticed.

We are much indebted to L.V. Interrante for supplying the TTF–AuBDT samples, and to I.S. Jacobs for inviting us to join the studies of the SP-problem. Stimulating discussions with him and with I.A. Northby and J.C. Bonner are gratefully acknowledged: The invaluable assistance of G.J. Kramer and R. Steeman in the experiments on TTF–AuBDT is also gratefully acknowledged. This work is part of the research program of the "Stichting voor Fundamenteel Onderzoek der Materie", which is sponsored by the "Nederlandse Organisatie voor Zuiver Wetenschappelijk Onderzoek".

[1] L.J. de Jongh and H.J.M. de Groot, Solid State Commun. 53 (1985) 731, 737, 56 (1985) 7.
[2] H.J.M. de Groot and L.J. de Jongh, submitted to Physica.
[3] J.A. Northby, H.A. Groenendijk, L.J. de Jongh, J.C. Bonner, I.S. Jacobs and L.V. Interrante, Phys. Rev. B25 (1982) 3215.
[4] J.A. Northby, F.J.A.M. Greidanus, W.J. Huiskamp, L.J. de Jongh, I.S. Jacobs and L.V. Interrante, J. Appl. Phys. 53 (982) 8032.
[5] T.W. Hijmans, W.H. Korving, G.J. Kramer, H.B. Brom, L.J. de Jongh, I.S. Jacobs and L.V. Interrante, Mol. Cryst. Liq. Cryst. 120 (1985) 251.
[6] T.W. Hijmans, H.B. Brom and L.J. de Jongh, Phys. Rev. Lett. 54 (1985) 1714.
[7] See e.g. Y. Shapira, N.F. Oliveira Jr. and S. Foner, Phys. Rev. B30 (1984) 6639.
[8] K. Binder and D.P. Landau, Phys. Rev. B13 (1976) 1140.
[9] D.P. Landau and K. Binder, Phys. Rev. B24 (1981) 1391.
[10] L.J. de Jongh, L.P. Regnault, J. Rossat-Mignod and J.Y. Henry, J. Appl. Phys. 53 (1982) 7963.
[11] J.W. Schutter, J.W. Metselaar and D. de Klerk, Physica 61 (1972) 250. K. Koyama, K. Amaya and K. Takeda, J. Magn. Magn. Mat. 31–34 (1983) 1196.
[12] G.P. Gupta, D.P.E. Dickson and C.E. Johnson, J. Phys. C12 (1979) 2411. Q.A. Pankhurst, C.E. Johnson and M.F. Thomas, J. Phys. C18 (1985) 3249.
[13] Y. Imry and M. Wortis, Phys. Rev. B19 (1979) 3580.
[14] For recent reviews see e.g. G. Grinstein, J. Appl. Phys. 55 (1984) 2371 or J. Villain, NATO-ASI on Scaling Phenomena in Disordered Systems, Geilo, Norway (1985) Plenum, to appear.
[15] A. Houghton, R.D. Kenway and S.C. Ying, Phys. Rev. B23 (1981) 298. J.L. Cardy and S. Ostlund, Phys. Rev. B25 (1982) 6899.
[16] K. Takeda, T. Koibe, T. Tonegawa and I. Harada, J. Phys. Soc. Japan 48 (1980) 1115, and references cited therein.
[17] J.P. Boucher, L.P. Regnault, J. Rossat-Mignod, J.P. Renard, J. Bouillot and W.J. Stirling, J. Appl. Phys. 52 (1981) 1956.
[18] L.J. de Jongh, J. Appl. Phys. 53 (1982) 8018.
[19] D. Bloch, J. Voiron and L.J. de Jongh, in: High-Field Magnetism, ed. M. Date (North-Holland, Amsterdam, 1983) p. 19.
[20] A.d. Bruce and D.J. Wallace, J. Phys. A16 (1983) 1721.
[21] A.I. Buzdin and L.N. Bulaevskii, Sov. Phys. Usp. 23 (1980) 409.
[22] J.W. Bray, L.V. Interrante, I.S. Jacobs and J.C. Bonner, in: Extended Linear Chain Compounds, vol. 3, ed. J.C. Miller (Plenum, New York, 1982) p. 353.
[23] L.J. de Jongh, Magneto-structural correlations in exchange-coupled systems, ed. R.D. Willett et al. (Reidel, Dordrecht, 1985) p. 1.
[24] T. Nakano and H. Fukuyama, J. Phys. Soc. Japan 49 (1980) 1679.
[25] B. Horovitz, Phys. Rev. Lett. 46 (1981) 742.
[26] I. Harada and A. Kotani, J. Phys. Soc. Japan 51 (1982) 1737.
[27] A.I. Buzdin, M.L. Kulić and V.V. Tugushev, Solid State Commun. 48 (1983) 483.
[28] M. Fukita and K. Machida, J. Phys. Soc. Japan 53 (1984) 4395.
[29] L.N. Bulaevskii, A.I. Buzdin and D.I. Khomskii, Solid State Commun. 27 (1978) 5.
[30] M.C. Cross, Phys. Rev. B20 (1979) 460.